

# A unitarity bound and the components of photon-proton interactions

E. Gotsman<sup>1,2</sup>, E.M. Levin<sup>1,2,3</sup>, U. Maor<sup>1</sup>

<sup>1</sup> School of Physics and Astronomy, Tel Aviv University, Ramat Aviv, 69978, Israel  
(e-mail: gotsman@post.tau.ac.il, leving@post.tau.ac.il, maor@post.tau.ac.il)

<sup>2</sup> DESY Theory, Notkestr. 85, D-22603, Hamburg, Germany

<sup>3</sup> Theory Department, Petersburg Nuclear Physics Institute, 188350, Gatchina, St. Petersburg, Russia

Received: 7 August 1997 / Revised version: 11 December 1997 / Published online: 10 March 1998

**Abstract.** We show how and why the short distance (“hard”) interaction, which is calculated in perturbative QCD, provides a mass cutoff in Gribov’s formula for photon-proton collisions. This enables us to find a new and more restrictive unitarity bound for this process,  $\sigma(\gamma^*p) \leq C(\ln \frac{1}{x})^{\frac{5}{2}}$ . We develop a simple model that consists of “soft” and “hard” contributions, which yields a qualitative description of the published experimental data over a wide range of photon virtualities ( $Q^2$ ) and energies ( $W$ ). This model provides a quantitative way of evaluating the relative rate of the short and long distance contributions, in the different kinematic regions. The main results of the analysis are (i) that even at  $Q^2 = 0$  and high energies the short distance contribution is not small, and it provides a possible explanation for the experimental rise of the photoproduction cross section; and (ii) at large values of  $Q^2$ , the long distance processes still contribute to the total cross section.

## 1 Introduction

The total cross section of a hadron-hadron interaction is bound by the Froissart-Martin limit [1]

$$\sigma_{tot} \leq C \ln^2 \frac{s}{s_0}, \quad (1)$$

where  $C = \frac{\pi}{\mu^2}$ , depends on the mass of the lightest particle exchanged in the crossed channel. The bound is a consequence of  $s$ -channel unitarity, analyticity and crossing symmetry. In spite of the ambiguity in the determination of  $C$ , we suggest that at the presently available hadron accelerator energies one should look for phenomena associated with  $s$ -channel unitarity, rather than the absolute bound. Indeed, a careful study [2] shows that the scale of saturation of  $s$ -channel unitarity in elastic  $\bar{p}p$  reactions is above the Tevatron energy, while the saturation scale for diffractive channels is considerably lower, appearing at ISR energies. This qualitative theoretical study is strongly supported by the experimental observation that, whereas  $\sigma_{el}/\sigma_{tot}$  grows all through the ISR-Tevatron range, the ratio  $\sigma_{diff}/\sigma_{tot}$  decreases with energy [3].

The study of unitarity and the Froissart-Martin bounds in DIS are more complicated than for the hadron-hadron case. These complications originate from ambiguities in the implementation of the unitarity constraints due to electromagnetic photon coupling and the absence of a proper elastic channel, as well as the introduction of the mass of the virtual photon as an additional kinematic

variable. From a phenomenological point of view, we have to take into account the “soft” and “hard”, or alternatively, the long distance and short distance phenomena, as contributors to the total  $\gamma^*p$  cross section, or the target structure function. This differs from the usual picture of the hadron-hadron collision, where the incoming time like particle masses are fixed, and the total cross section is determined by the “soft” (long distance) Pomeron.

A remarkable simplification of the DIS analysis has been suggested by Gribov [4] in the context of DIS on a nuclear target. Gribov’s main observation was that at high energies, the  $\gamma^*$  fluctuates into a hadronic system (i.e.  $\bar{q}q$  to the lowest order) with a coherence length,  $l_c = \frac{1}{m_x}$ , which is much larger than the target radius.  $m$  denotes the target mass and  $x$  the Bjorken scaling variable ( $x = \frac{Q^2}{s}$ , where  $Q^2$  is the photon virtuality). Hence, we can describe DIS as a two step process

- 1) The  $\gamma^*$  transforms into a hadronic system well before the interaction with the target.
- 2) The produced hadronic system interacts with the target.

Gribov added two technical assumptions, which simplified the calculation

- a) The hadronic interaction is a black disc interaction. This assumption was made for a heavy nuclear target. In the black disc limit, the strong interaction diffractive dissociation channels  $M^2p \rightarrow M'^2p$  with  $M \neq M'$  can be neglected.

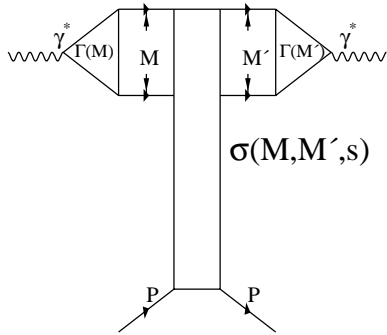


**Fig. 1.** The generalized Gribov's formula for DIS

b) A dispersion relation, without subtractions, can be written in terms of the variable  $M^2$ .

The resulting DIS cross section is then written as

$$\sigma(\gamma^* N) = \frac{\alpha_{em}}{3\pi} \int \frac{R(M^2) M^2 dM^2}{(Q^2 + M^2)^2} \sigma_{M^2 N}(s). \quad (2)$$

Here  $R(M^2)$  is defined as the ratio

$$R(M^2) = \frac{\sigma(e^+e^- \rightarrow \text{hadrons})}{\sigma(e^+e^- \rightarrow \mu^+\mu^-)}. \quad (3)$$

The notation is illustrated in Fig. 1 where  $M^2$  is the mass squared of the scattered hadronic system,  $\Gamma^2(M^2) = R(M^2)$  and  $\sigma_{M^2 N}(s)$  is the cross section for the hadronic system to scatter off the nucleonic target.

Assuming (1) for  $\sigma_{M^2 N}$  and integrating (2) over  $M^2$  we obtain a  $\gamma^* p$  cross section which behaves like  $\ln(\frac{M_{max}^2 + Q^2}{M_{min}^2 + Q^2})$ . We note that  $M_{min}^2 = 4m_\pi^2$ , whereas  $M_{max}^2 \propto s$ , therefore, one easily obtains the Gribov's bound [5]

$$\sigma(\gamma^* N) \leq \frac{\alpha_{em}}{3\pi} R_\infty C \ln^2 \frac{s}{s_0} \ln \frac{1}{x}, \quad (4)$$

here  $R_\infty$  denotes the ratio given by (3) in the high energy limit. The logarithmic behaviour of the above bound is unchanged by the introduction of an arbitrary high mass cutoff  $\frac{M^2}{s} \leq 0.1$  [5]. A disturbing feature of (4), is that it is less stringent than the Froissart-Martin bound, and we question whether this is a genuine feature of DIS, or an artifact of our approach and the assumed input. In particular, an extra logarithmic power of  $M^2$  which appears in (2) due to the upper limit of the integration, does not appear explicitly in Gribov's formula.

Attempting to clarify these problems, we present a calculation that maintains Gribov's basic hypothesis, which we find attractive, but gives up the black disc assumption for large values of  $M^2$ . The physical reason why the black disc assumption cannot be correct, even for a very heavy nucleus, or at extremely high energies in the Froissart-Martin region, is simple. The quark-antiquark pair with a large mass has a small transverse size, typically of the order of  $r_\perp \propto \frac{1}{M}$ . Being colour neutral such a pair can penetrate without interacting through a large target such as a heavy nucleus, or a hadron at ultra high energies.

The attractive feature of this scenario is that at large  $M^2$  the interaction takes place at small distances, or in other words, it is a hard process which can be calculated in the framework of perturbative QCD (pQCD).

In Sect. 2 we develop a general method to take into account the effect described above, and show that (4) should be replaced by the following relation:

$$\sigma(\gamma^* N) \leq \frac{\alpha_{em}}{3\pi} R_\infty C \ln^2 \frac{s}{s_0} \ln\left(\frac{Q^2 + M^2(x)}{Q^2 + M_0^2}\right), \quad (5)$$

where  $M^2(x)$  is the solution of the equation

$$\frac{4\pi\alpha_S}{3R_N^2 M^2(x)} x G^{DGLAP}(x, M^2(x)) = 1. \quad (6)$$

$xG$  denotes the gluon density of the target, and  $R_N^2$  the gluon correlation radius, that has been estimated using the HERA diffractive dissociation data in [6].  $M_0^2$  is a cutoff in mass that separates the "soft" (long distance) processes from the "hard" (short distance) ones. Clearly, the assumption that the production for  $M^2 < M_0^2$  is soft, whereas  $M^2 \geq M_0^2$  is hard, is an oversimplification. In our approach, the value of  $M_0^2$  is a pure phenomenological parameter, which we determine from a fit to the experimental DIS data at sufficiently small values of  $Q^2$ .

In Sect. 3 we develop a phenomenological approach based on our general formulae of Sect. 2, that allows us to match the DIS and real photoproduction data. The main idea underlying our approach is to parameterize the low mass region using Gribov's formula for the "soft" processes, while for the high  $M^2$  contribution, the leading  $\alpha_S \ln(1/x)$  approximation of pQCD is used. We show that with the choice  $M_0^2 \approx 5 \text{ GeV}^2$ , we are able to qualitatively describe the main features of the experimental data for photon nucleon interactions at high energy, and for most values of the photon virtuality ( $Q^2$ ).

## 2 General formalism and a Gribov-Froissart type bound for DIS

### 2.1 A generalization of the Gribov's formula

As mentioned above, Gribov argued that one can use a dispersion relation with respect to the masses  $M$  and  $M'$  to describe the photon-hadron interaction (see Fig. 1 for notation), as the correlation length  $l_c = \frac{1}{mx} \gg R_N$ , the target size. Based on this idea we can write a general formula for the photon-hadron interaction,

$$\sigma(\gamma^* N) = \frac{\alpha_{em}}{3\pi} \int \frac{\Gamma(M^2) dM^2}{Q^2 + M^2} \times \sigma(M^2, M'^2, s) \frac{\Gamma(M'^2) dM'^2}{Q^2 + M'^2}. \quad (7)$$

In the black disc approximation  $\sigma(M^2, M'^2, s) = 2\pi R_N^2 M^2 \delta(M^2 - M'^2)$ , which leads to the Gribov's formula of (2). Equation (7) enables us to

separate the “soft” and “hard” interactions, by introducing a separation scale  $M_0$  in the integral over the masses  $M$  and  $M'$  in (7). Equation (7) can be rewritten in the form

$$\sigma(\gamma^* N) = \sigma^{soft} + \sigma^{hard}, \quad (8)$$

where

$$\begin{aligned} \sigma^{soft} &= \frac{\alpha_{em}}{3\pi} \int_{4m_\pi^2}^{M_0^2} \frac{\Gamma(M^2) dM^2}{Q^2 + M^2} \\ &\quad \times \sigma(M^2, M'^2, s) \frac{\Gamma(M'^2) dM'^2}{Q^2 + M'^2} \\ &\leq \frac{\alpha_{em}}{3\pi} \int_{4m_\pi^2}^{M_0^2} \frac{R(M^2) M^2 dM^2}{(Q^2 + M^2)^2} \sigma_{M^2 N}(s). \end{aligned} \quad (9)$$

Here, we have used Gribov’s ideas to estimate the contribution of the “soft” processes using the black disc approximation. It would be preferable if the “soft” contribution could be calculated in nonperturbative QCD (npQCD). Thus far, unfortunately, no consistent npQCD approach has been developed for this contribution and what we have at hand are only phenomenological parameterizations describing the “soft” hadron processes. We observe that experimentally  $\frac{\sigma_{diff}}{\sigma_{el}}$  is decreasing rapidly with energy in nucleon-nucleon interactions [3]. In our context this translates to the observation that a transition from a hadronic system with mass  $M$  to one with mass  $M'$  is somewhat smaller than the elastic cross section which does not change the value of the mass. Moreover, we expect theoretically the ratio  $\frac{\sigma_{diff}}{\sigma_{el}}$  to decrease logarithmically in the high energy limit [2]. These observations support our idea that a suppression of  $M$  to  $M'$  transition can be used as the first order estimate of the “soft” contribution in (7). Clearly, at this stage, any description of the “soft” term in (8) has to be based on a model.

An attractive feature of our approach is the introduction of the separation scale  $M_0$ . This allows us to use both the “soft” high energy phenomenology as well as the pQCD calculation for the photon-hadron interaction at high energy.

Accordingly, for the short distance contributions we have

$$\begin{aligned} \sigma^{hard} &= \frac{\alpha_{em}}{3\pi} \int_{M_0^2}^{\infty} \frac{\Gamma(M^2) dM^2}{Q^2 + M^2} \\ &\quad \times \sigma^{QCD}(M^2, M'^2, s) \frac{\Gamma(M'^2) dM'^2}{Q^2 + M'^2}, \end{aligned} \quad (10)$$

where we can use the leading  $\alpha_S \ln(\frac{1}{x})$  approximation of pQCD to evaluate this integral.

## 2.2 The “hard” contribution to the generalized Gribov’s formula

We wish to rewrite the formula for the “hard” DIS cross section in a form which is similar to (10). The cross section

for DIS in the region of small  $x$  (high energy) in the leading  $\alpha_S \ln(\frac{1}{x})$  approximation of pQCD, has the form [7, 8]

$$\begin{aligned} \sigma_{\gamma^* p}^{QCD} &= \int_0^1 dz \int d^2 r_\perp |\Psi^{\gamma^*}(Q^2, z, r_\perp)|^2 \\ &\quad \times \int d^2 b_t \sigma_N(x, r_\perp, b_t), \end{aligned} \quad (11)$$

where  $\Psi^{\gamma^*}$  is the wave function of the virtual photon. Although the separation between the “soft” and “hard” sectors is more natural in the analysis of longitudinal polarized photons<sup>1</sup>, we limit our discussion at this stage to transverse polarized photons as this gives the dominant contribution to the total cross section. The calculations pertaining to the longitudinal polarized photons will be published elsewhere.

For a transverse polarized photon we have [9]

$$\begin{aligned} |\Psi_T^{\gamma^*}|^2 &= \frac{\alpha_{em} N_c}{2\pi^2} \sum_f Z_f^2 [z^2 + (1-z)^2] \\ &\quad \times \bar{Q}^2 K_1^2(\bar{Q} r_\perp), \end{aligned} \quad (12)$$

where  $K_1$  is the modified Bessel function,  $\bar{Q}^2 = Q^2 z(1-z)$ , and  $N_c$  the number of colours.  $Z_f$  and  $z$  are the fraction of the charge, and the fraction of energy carried by the quark.  $r_\perp$  denotes the transverse splitting between the quark and antiquark.  $\sigma_N(x, r_\perp, b_t)$  is the cross section of the colour dipole of a size  $r_\perp$  with the target at fixed impact parameter  $b_t$ . This cross section is equal to

$$\sigma_N(x, r_\perp, b_t) = 2 \text{Im} a_{el}(x, r_\perp, b_t), \quad (13)$$

where  $a_{el}$  is the elastic amplitude in the  $b_t$ -representation, which is closely related to the scattering amplitude of the dipole at a definite value of the transfer momentum squared  $t = -q_t^2$

$$a_{el}(x, r_\perp, b_t) = \frac{1}{2\pi} \int d^2 q_t e^{-i\mathbf{q}_t \cdot \mathbf{b}_t} A(x, r_\perp, t). \quad (14)$$

Since high energy experimental data suggest that  $\text{Re} a_{el} \ll \text{Im} a_{el}$ ,  $s$ -channel unitarity implies [7, 8]

$$\sigma_N(x, r_\perp, b_t) = 2 \{1 - e^{-\frac{1}{2}\Omega}\}, \quad (15)$$

with arbitrary real function  $\Omega$ . In the kinematic region where  $\Omega \ll 1$ , for dipoles of small sizes  $r_\perp \ll R_N$ , this function is equal to [10]

$$\Omega = S(b_t) \frac{\pi^2 \alpha_S}{3} r_\perp^2 x G(x, \frac{4}{r_\perp^2}). \quad (16)$$

$S(b_t)$  is the nonperturbative two gluon form factor, which normalizes as  $\int d^2 b_t S(b_t) = 1$ . From general principles of analyticity we only know its large  $b_t$  behaviour,  $S(b_t)|_{b_t \rightarrow \infty} \rightarrow e^{-2\mu b_t}$ , where  $\mu$  is the mass of the lightest hadron (pion).

<sup>1</sup> This subject will be further discussed in Sect. 3

Many practical applications assume an exponential parameterization for  $S(b_t)$  of the form

$$S(b_t) = \frac{1}{\pi R_N^2} e^{-\frac{b_t^2}{R_N^2}}, \quad (17)$$

where  $R_N^2$  is the correlation length between two gluons in the proton. For the case of uncorrelated gluons  $R_N$  is the hadron (proton) radius.

We wish to comment on the form of (16), recalling the standard procedure for solving the DGLAP evolution equations.

1) The first step: we introduce the moments of the parton density,

$$xG(x, Q^2) = \frac{1}{2\pi i} \int_C e^{-\omega \ln(1/x)} M(\omega, Q^2) d\omega,$$

where the contour  $C$  is located to the right of all the singularities of the moment  $M(\omega, Q^2)$ .

2) The second step: we find the solution to the DGLAP equations for the moment

$$\frac{dM(\omega, Q^2)}{d \ln Q^2} = \gamma(\omega) M(\omega, Q^2). \quad (18)$$

The solution is

$$M(\omega, Q^2) = M(\omega, Q_0^2) e^{\gamma(\omega) \ln(Q^2/Q_0^2)}. \quad (19)$$

Here  $M(\omega, Q_0^2)$  is the nonperturbative input which is taken either from experimental data or from the ‘‘soft’’ (model dependent) phenomenology.

3) The third step: we find the solution for the parton density using the inverse transform

$$xG(x, Q^2) = \int_C \frac{d\omega}{2\pi i} e^{\omega \ln(1/x) + \gamma(\omega) \ln(Q^2/Q_0^2)} \times M(\omega, Q_0^2). \quad (20)$$

We conclude that in order to find a solution of the DGLAP equation we need to know the nonperturbative input  $M(\omega, Q_0^2)$  and the anomalous dimension  $\gamma(\omega)$ , which we can calculate in pQCD. To obtain the  $b_t$ -dependence of the deep inelastic structure function we have to calculate the  $t$ -dependence of the imaginary part of the virtual photon Compton amplitude (see (13) and (14)). In the framework of the DGLAP evolution equations we have two different regions of  $t$ : (i)  $t \leq Q_0^2$  and (ii)  $t \geq Q_0^2$ . For the case when  $t \geq Q_0^2$ ,  $t$  defines the factorization scale and replaces  $Q_0^2$  in (20) (see [11]). However, for  $t \leq Q^2$  the factorization scale is equal to  $Q_0^2$  and the only  $t$ -dependence is concentrated in  $M(\omega, Q_0^2; t)$ . The factorizable form of the initial moments  $M(\omega, Q_0^2; t) = M(\omega, Q_0^2) F(t)$  is certainly an assumed model, but this model is reasonable for  $t \ll Q_0^2$ . It should be stressed that this assumption which led to the explicit form of (16), is not needed for the large  $b_t$  behaviour, which is the only ingredient of (16) used for the proof of the Gribov-Froissart bound for DIS.

Using (15), we can distinguish between two kinematic limits that we use for our approximation.

I)  $\Omega \ll 1$  and  $\sigma_N(x, r_\perp, b_t) \rightarrow \Omega$  with  $\Omega$  given by (16).

II)  $\Omega \gg 1$  where  $\sigma_N(x, r_\perp, b_t) = 2 \{1 - e^{-\frac{1}{2}\Omega}\} \rightarrow 2$ .

At each fixed  $x$  and  $r_\perp$  the boundary between these two regions occurs at  $b_t = b_0$ , which can be determined from the equation

$$S(b_0) \frac{\pi^2 \alpha_S}{3} r_\perp^2 xG(x, \frac{4}{r_\perp^2}) = 1. \quad (21)$$

Substituting the large  $b_t$  behaviour of the form factor  $S(b_t)$ , one finds

$$b_0 = \frac{1}{2\mu} \ln[r_\perp^2 xG(x, \frac{4}{r_\perp^2})]. \quad (22)$$

In the kinematic region II we rewrite (11) in the form of (10). This is a very simple task once we recall that

$$\bar{Q}K_1(\bar{Q}r_\perp) = \int \frac{k^2 dk}{\bar{Q}^2 + k^2} J_0(kr_\perp), \quad (23)$$

or

$$[\bar{Q}K_1(\bar{Q}r_\perp)]^2 = \int \frac{k_1^2 dk_1}{\bar{Q}^2 + k_1^2} J_0(k_1 r_\perp) \times \int \frac{k_2^2 dk_2}{\bar{Q}^2 + k_2^2} J_0(k_2 r_\perp). \quad (24)$$

Using the simple form of  $\sigma_N(x, r_{perp}, b_t) = 2$  in region II, one can integrate (11) over  $k_2$  and  $z$  introducing a new variable  $M^2 = \frac{k_1^2}{z(1-z)}$ . We obtain

$$\sigma_{\gamma^* p}^{QCD} = \frac{\alpha_{em} 2N_c}{3\pi^2} \sum_f Z_f^2 \times \int_{M_0^2}^\infty \frac{M^2 dM^2}{(Q^2 + M^2)^2} \pi \int_0^{b_0^2} db_t^2. \quad (25)$$

At first sight it appears that there is no natural cutoff in the above  $M^2$  integration, but as we shall see later this is not so.

### 2.3 The unitarity bound on the photon cross section

To obtain the unitarity bound for the total cross section of the photon-nucleon interaction, we use the decomposition of (8) and Gribov's estimates for  $\sigma^{soft}$  given in (9). For  $\sigma_{M^2 N}(s)$  in (9) we can apply the Froissart-Martin bound of (1), since it is a typical hadronic (on mass shell) cross section. Note, that the Froissart-Martin bound is a high energy limit for which the Gribov black disc assumption is perfectly adequate since the diffractive ( $M \neq M'$ ) channels are suppressed relative to the elastic ( $M = M'$ ) channel. We can evaluate  $\sigma^{hard}$  in (8) using the inequality  $\sigma^{hard} \leq \sigma^{QCD}$  where  $\sigma^{QCD}$  is determined by (25). We wish to explore further the nature of the upper limit of

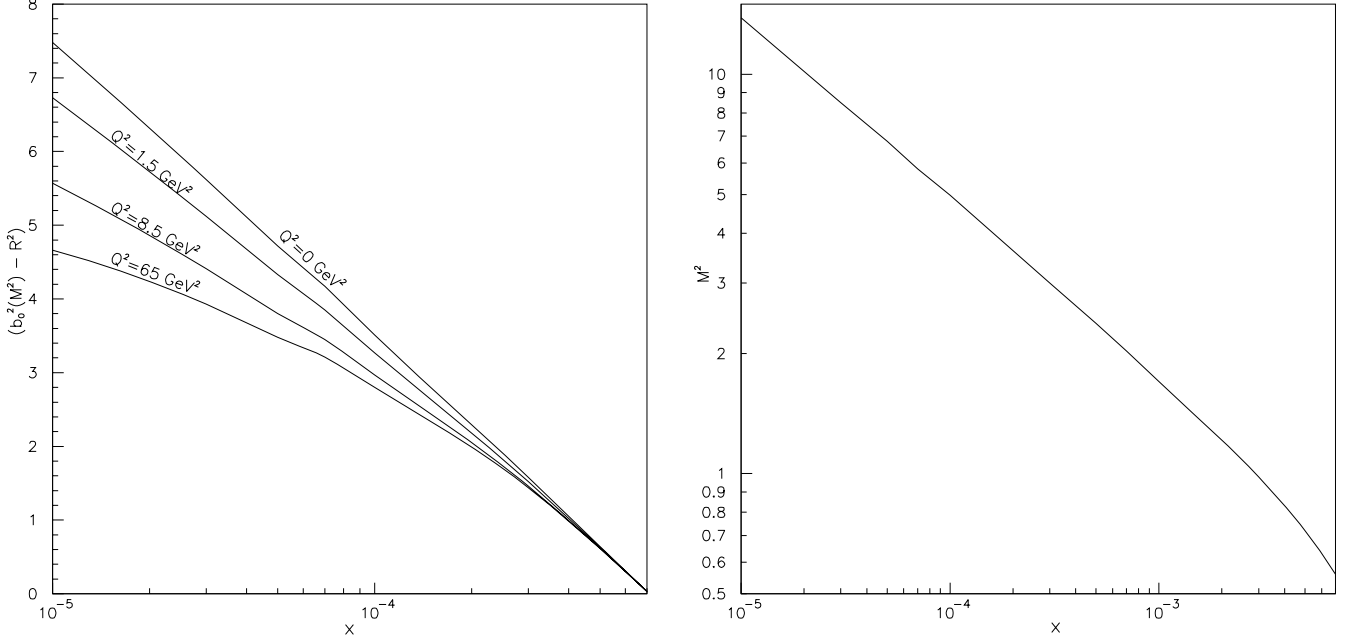


**Fig. 2.** Solutions of (21) ( $b_0^2(x)$ ) and of (30) ( $M^2(x)$ ), using the GRV parameterization [16] for the gluon structure function

the integration with respect to  $M^2$  in (25). To do this we return to (21). This equation has no solution if

$$S(b_t = 0) \frac{\pi^2 \alpha_S}{3} r_\perp^2 x G(x, \frac{4}{r_\perp^2}) < 1. \quad (26)$$

Therefore, the main contribution to  $\sigma_{\gamma^* p}^{QCD}$  in (11) comes from the kinematic region II with  $r_\perp^2 > r_0^2(x)$ , where  $r_0^2(x)$  is a solution of the equation

$$S(b_t = 0) \frac{\pi^2 \alpha_S}{3} r_0^2(x) x G(x, \frac{4}{r_0^2(x)}) = 1. \quad (27)$$

Using the notation  $S(b_t = 0) = \frac{1}{\pi R_N^2}$  (see (17)), (27) can be rewritten in a more familiar form

$$\frac{\pi \alpha_S}{3 R_N^2} r_0^2(x) x G(x, \frac{4}{r_0^2(x)}) = 1. \quad (28)$$

Due to the uncertainty principle

$$r_\perp^2 \propto \frac{1}{k_\perp^2} = \frac{1}{M^2 z(1-z)}. \quad (29)$$

As the integration<sup>2</sup> over  $z$  in (11) is convergent in the limit  $\sigma_N(x, r_{perp}, b_t) = 2$  (see (24) and (25)), we can safely put  $z = \frac{1}{2}$  in (29)<sup>3</sup>, and rewrite (28) as an equation for the upper limit of the integration over  $M^2$

$$\frac{4\pi \alpha_S}{3 R_N^2 M^2(x)} x G(x, M^2(x)) = 1. \quad (30)$$

<sup>2</sup> We will comment on the  $z$ -integration in the ‘‘hard’’ cross section for  $\Omega \ll 1$  later

<sup>3</sup> It means that  $r_\perp \propto \frac{2}{M}$ . This fact justifies our main input of a separation scale ( $M_0$ ) in Gribov’s formula of (7)

Collecting all contributions we find

$$\begin{aligned} \sigma(\gamma^* N) \leq \frac{\alpha_{em}}{3\pi} \left\{ C \ln^2 \frac{s}{s_0} \int_{4m_\pi^2}^{M_0^2} \frac{R(M^2) M^2 dM^2}{(Q^2 + M^2)^2} \right. \\ \left. + 2R_\infty b_0^2 \ln \left( \frac{Q^2 + M^2(x)}{Q^2 + M_0^2} \right) \right\}. \quad (31) \end{aligned}$$

This equation provides an improved Gribov-Froissart bound for the photon-hadron total cross section, in place of the less restrictive one given in (4). For very small  $x$  (30) leads to  $M^2(x) \rightarrow \Lambda^2 \exp(\sqrt{a \ln(1/x)})$ , where  $\Lambda$  is the QCD scale and the constant  $a$  has been calculated in [11]. This implies that for very small  $x$ , the bound for  $\sigma(\gamma^* N)$  at  $Q^2 < M^2(x)$  is

$$\begin{aligned} \sigma(\gamma^* N) \leq \frac{\alpha_{em}}{3\pi} 2R_\infty \left[ \sqrt{a \ln(1/x)} - \ln(Q^2/\Lambda^2) \right] \\ \times C \ln^2 \frac{s}{s_0}. \quad (32) \end{aligned}$$

In the ultra small  $x$  limit we obtain that  $\sigma(\gamma^* N) \leq C' (\ln(\frac{1}{x}))^{\frac{5}{2}}$  where  $C'$  contains all relevant constants.

## 2.4 Numerical estimates for the behaviour of $\sigma(\gamma^* N)$

We can use (31) also to make numerical estimates of the high energy behaviour of the DIS total cross section. For this purpose we rewrite (31) and attempt to evaluate  $\sigma_{M^2 N}$  of (9) rather than using its high energy bound. To this end we assume

$$\begin{aligned} \sigma(\gamma^* N) \leq \frac{\alpha_{em}}{3\pi} \left\{ \sigma_{hadron}^{soft}(s) \int_{4m_\pi^2}^{M_0^2} \frac{R(M^2) M^2 dM^2}{(Q^2 + M^2)^2} \right. \\ \left. + 2R_\infty b_0^2 \ln \frac{Q^2 + M^2(x)}{Q^2 + M_0^2} \right\}, \quad (33) \end{aligned}$$

where  $\sigma_{hadron}^{soft}(s)$  is a typical cross section for a meson-nucleon interaction. To obtain an estimate, we take  $\sigma_{hadron}^{soft}(s) = \frac{1}{2}(\sigma(\pi^+p) + \sigma(\pi^-p))$ , and use the Donnachie-Landshoff parameterization [14] for its energy behaviour.

Solutions of (21) (i.e.  $b_0^2(x)$ ) and of (30) (i.e.  $M^2(x)$ ) are plotted in Fig. 2, using the GRV parameterization [16] for the gluon density. In solving (21), we have used (17), with  $R_N^2 = 10 GeV^2$ . The value of  $R_N^2$  is derived from HERA data on diffractive production of vector mesons in DIS, and from the high energy phenomenology for “soft” processes (see [6] for details). We need to calculate  $b_0^2$  at fixed  $x$  for all values of  $M^2 \leq M^2(x)$ . However, since the integral over  $M^2$  is logarithmic, we can evaluate its contribution at an average  $\bar{M}^2$ .  $\bar{M}^2$  is determined from the relation  $\int_{M_0^2}^{\bar{M}^2} \frac{dM^2}{Q^2 + M^2} = \int_{\bar{M}^2}^{M^2(x)} \frac{dM^2}{Q^2 + M^2}$ , which gives  $\bar{M}^2 = \sqrt{(Q^2 + M^2(x))(Q^2 + M_0^2) - Q^2}$ .  $b_0^2$  at this mass value is plotted in Fig. 2. We consider the values, given in Fig. 2, to be more relevant at presently accessible energies, than the highly asymptotic Froissart-like estimates.

Figure 3 shows the energy dependence of the r.h.s. of (33) together with the experimental data. The values of  $M^2(x)$  (see Fig. 2b) show that we can trust our estimate, given by (33), only for  $x \leq 10^{-3}$ . This means that we can compare our bound only with the available experimental data at relatively small values of  $Q^2$ . We plot the data and our estimates from (33) only at  $Q^2 \approx 0$ , since for quasi real photoproduction we reach the smallest values of  $x$ . One should note that (33) was proven only at very small  $x$ , where we can neglect the contribution from the kinematic region where  $\Omega \ll 1$  (region I). Actually, in the HERA kinematic region at all available  $Q^2$  and  $W$ , we cannot neglect the contribution from region I. On the other hand, Fig. 3 shows that our bound is rather close to the experimental data for real photoproduction. This suggests that (33) reflects the main physics for the HERA kinematic region. We expect that the inclusion of the “hard” contribution from kinematic region I, will improve our estimates, but will not produce a dramatic change.

### 3 Matching of the “soft” and “hard” processes in DIS

#### 3.1 General description

In the following we develop a phenomenological approach to describe DIS at all values of  $Q^2$  based on the separation of the “soft” and “hard” interactions, in the framework of the Gribov formula (see (7) and (8)). This approach provides a relatively simple description, in which the mass integration with  $M^2 < M_0^2$  is controlled by the “soft” interaction. For  $M^2 > M_0^2$  we are dealing with a “hard” interaction, which we can treat in pQCD. For  $\sigma^{soft}$  in (8) we assume that the “soft” high energy strong interaction suppresses the diffractive dissociation of a hadron state of mass  $M$  to a hadron state with a different mass  $M'$ . This property is true, for example, in the additive constituent quark model, where the interaction of the hadron can be reduced to an interaction of the quarks, namely, only the

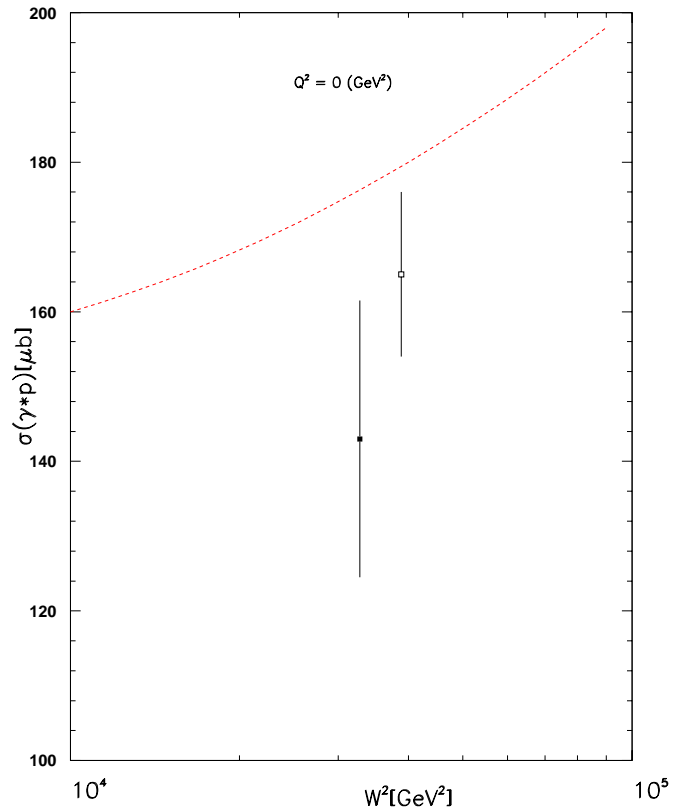


Fig. 3. The energy dependence of the r.h.s. of (33) together with the experimental data

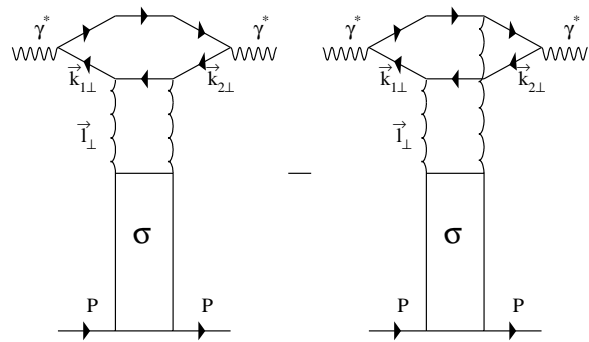


Fig. 4. The diagrams for two gluon exchange model

first diagram of Fig. 4 (with  $M = M'$ ), contributes. In a different context this is also a consequence of the implementation of screening corrections [11]. With this assumption, we can rewrite the “soft” contribution in the form

$$\sigma^{soft} = \frac{\alpha_{em}}{3\pi} \int_{4m_\pi}^{M_0^2} \frac{R(M^2) M^2 dM^2}{(Q^2 + M^2)^2} \sigma_{M^2 N}(s). \quad (34)$$

For  $\sigma^{hard}$  we use the general formula of (10), where  $\sigma^{QCD}(M^2, M'^2, s)$  is rewritten in terms of the gluon-nucleon interaction in the framework of a two gluon exchange model, shown in Fig. 4. This model is certainly correct in the region of very small  $x$  ( $\alpha_S \ln(1/x) \geq 1$ ) and large  $M^2$  ( $\alpha_S \ln(M^2/\Lambda^2) \geq 1$ ), and it also reflects the main

properties of the QCD interaction outside this particular kinematic region.

We shall discuss the assumptions made for  $\sigma^{soft}$  and (34) later. Prior to that we wish to specify the well known “hard” contribution. This will also be instructive for our discussion of the “soft” contribution in Sect. 3.3.

### 3.2 The two gluon exchange model

Equation (11) is the basic formula for the two gluon exchange model, where we use the following representation for  $\sigma(x, r_\perp) = \int d^2 b_t \sigma_N(x, r_\perp, b_t)$

$$\sigma(x, r_\perp) = \int d^2 l_\perp \sigma(l_\perp^2) \{1 - e^{i\mathbf{l}_\perp \cdot \mathbf{r}_\perp}\}. \quad (35)$$

One can easily see that the two terms in (35) just reflect the two diagrams in Fig. 4.

Substituting (35) in (11) and using (24), we obtain

$$\begin{aligned} \sigma^{hard} &= \frac{\alpha_{em} N_c}{2\pi^2} \sum_f Z_f^2 \int_0^1 dz [z^2 + (1-z)^2] \\ &\times \left\{ \int \frac{d^2 k_{1\perp} d^2 k_{2\perp}}{(\bar{Q}^2 + k_{1\perp}^2)^2} \int_0^\infty \sigma(l_\perp^2) dl_\perp^2 \right. \\ &- \int \frac{d^2 k_{1\perp} d^2 k_{2\perp} \mathbf{k}_{1\perp} \cdot \mathbf{k}_{2\perp}}{(\bar{Q}^2 + k_{1\perp}^2)(\bar{Q}^2 + k_{2\perp}^2)} \\ &\left. \times \sigma(l_\perp^2 = (\mathbf{k}_{1\perp} - \mathbf{k}_{2\perp})^2) \right\} \quad (36) \end{aligned}$$

In (36) we integrate over the angle between  $\mathbf{k}_{1\perp}$  and  $\mathbf{l}_\perp$  and introduce a new variable  $\tilde{M}$

$$\begin{aligned} M^2 &= \frac{k_{1\perp}^2}{z(1-z)}; \\ M'^2 &= \frac{k_{2\perp}^2}{z(1-z)}; \\ \tilde{M}^2 &= \frac{l_\perp^2}{z(1-z)}. \end{aligned} \quad (37)$$

The physical meaning of  $\tilde{M}$  is clear. Indeed, on the average

$$\begin{aligned} |M^2 - M'^2| &= \left| \frac{k_{1\perp}^2}{z(1-z)} - \frac{(\mathbf{k}_{1\perp} - \mathbf{l}_\perp)^2}{z(1-z)} \right| \\ &= \frac{-2\mathbf{k}_{1\perp} \cdot \mathbf{l}_\perp + l_\perp^2}{z(1-z)} = \langle \tilde{M}^2 \rangle. \end{aligned}$$

In terms of the new variables, (36) has the form

$$\begin{aligned} \sigma^{hard} &= \frac{\alpha_{em}}{4\pi^2} \int_0^1 dz [z^2 + (1-z)^2] \\ &\times \int dl_\perp^2 \int_{M_0^2}^\infty \frac{R(M^2) dM^2}{Q^2 + M^2} \left\{ \frac{M^2 - Q^2}{M^2 + Q^2} \right. \\ &\left. + \frac{Q^2 + \tilde{M}^2 - M^2}{\sqrt{(Q^2 + M^2 + \tilde{M}^2)^2 - 4M^2 \tilde{M}^2}} \right\} \sigma(l_\perp^2). \quad (38) \end{aligned}$$

Note that (38) applies in the region  $M^2 > M_0^2$  and that  $R(M^2)$  replaces  $R_\infty = N_c \sum_f Z_f^2$ .

Since  $z(1-z) = \frac{l_\perp^2}{M^2}$ , (38) can be rewritten in the form

$$\begin{aligned} \sigma^{hard} &= \frac{\alpha_{em}}{4\pi^2} \int_{4m_\pi}^\infty \frac{d\tilde{M}^2}{\tilde{M}^4} \int_{M_0^2}^\infty \frac{R(M^2) dM^2}{Q^2 + M^2} \\ &\times \int_{Q_0^2}^{\frac{\tilde{M}^2}{4}} \left[ 1 - 2\frac{l_\perp^2}{M^2} \right] l_\perp^2 dl_\perp^2 \sigma(l_\perp^2) \frac{1}{\sqrt{1 - \frac{4l_\perp^2}{M^2}}} \\ &\times \left\{ \frac{M^2 - Q^2}{M^2 + Q^2} \right. \\ &\left. + \frac{Q^2 + \tilde{M}^2 - M^2}{\sqrt{(Q^2 + M^2 + \tilde{M}^2)^2 - 4M^2 \tilde{M}^2}} \right\}. \quad (39) \end{aligned}$$

Recalling that  $\sigma(l_\perp^2) = \alpha_S(l_\perp^2) \frac{\phi(l_\perp^2)}{l_\perp^2}$ , where  $\alpha_S(Q^2) xG(x, Q^2) = \int^{Q^2} \alpha_S(l^2) \phi(l^2) dl^2$  (see [11] for details), we obtain, in the limit  $\frac{4l_\perp^2}{M^2} \ll 1$ , that

$$\begin{aligned} \sigma^{hard} &= \frac{\alpha_{em}}{3\pi} 2\pi^2 \int_{M_0^2}^\infty \frac{dM^2 R(M^2)}{Q^2 + M^2} \int_{4Q_0^2}^\infty \frac{d\tilde{M}^2}{\tilde{M}^4} \\ &\times \alpha_S \left( \frac{\tilde{M}^2}{4} \right) xG \left( x, \frac{\tilde{M}^2}{4} \right) \left\{ \frac{M^2 - Q^2}{M^2 + Q^2} \right. \\ &\left. + \frac{Q^2 + \tilde{M}^2 - M^2}{\sqrt{(Q^2 + M^2 + \tilde{M}^2)^2 - 4M^2 \tilde{M}^2}} \right\}. \quad (40) \end{aligned}$$

This equation is our master formula for the evaluation of the “hard” contribution (with light quarks) to the total photon-nucleon cross section.  $Q_0^2$  is the starting value of the gluon virtuality for the DGLAP evolution equations.

We wish to add two comments concerning the above master equation.

1)  $z$  has the same value before and after the interaction. This is a direct manifestation of the leading log (1/x) approximation in which we only take into account contributions of the form  $(\alpha_S \ln(1/x))^n$ . To understand this we compare the time of the interaction of the  $q\bar{q}$ -pair with the target ( $\tau_i$ ) to the life time of the virtual photon fluctuating into a  $q\bar{q}$ -pair ( $\tau_{\gamma^*}$ ). According to the uncertainty principle

$$\tau_{\gamma^*} \sim \frac{1}{\Delta E} = \left| \frac{1}{q_- - k_{1-} - k_{2-}} \right| = \frac{z(1-z)q_+}{Q^2 + k_\perp^2}, \quad (41)$$

where  $k_1$  and  $k_2$  are the four momenta of quark (anti-quark) (see Fig. 4). An estimate of the interaction time can be obtained from the typical time for the emission of a gluon with momentum  $l$  from the quark  $k_1$ , (i.e., see the second diagram in Fig. 4).

$$\tau_i \sim \left| \frac{1}{k_{1-} - k'_{1-} - l_-} \right| = \left| \frac{q_+}{\frac{k_{1\perp}^2}{z} - \frac{k_{2\perp}^2}{z'} - \frac{l_\perp^2}{\alpha}} \right|, \quad (42)$$

where  $\alpha = \frac{l_{\perp}}{q_{\perp}}$  and  $z' = z - \alpha$ . In the leading  $\log(1/x)$  approximation we have  $\alpha \ll z$  and hence

$$\tau_i \approx \frac{\alpha q_{\perp}}{l_{\perp}^2} \ll \tau_{\gamma^*}. \quad (43)$$

Equation (43) shows explicitly that the processes of a virtual and/or real photon scattering off a target can be described as a two stage process: initially the photon decays into a  $q\bar{q}$ -pair and only a long time after that the pair interacts with the target. This is why such a process can be described by the Gribov's formula.

2) An important feature of (40) is the fact that we integrate over  $z$  using  $z(1-z) = \frac{l_{\perp}^2}{M^2}$ . The integral over  $l_{\perp}^2$  is logarithmic and the typical values of  $l_{\perp}^2$  are of the order of  $l_{\perp}^2 \approx \tilde{M}^2 \exp(-\frac{1}{\gamma})$  where  $\gamma$  is the anomalous dimension. Since we are interested in the region of small  $x$  where  $\gamma$  is rather large, one can see that the typical values of  $z$ , which are essential in our integration, turn out to be of the order of unity. As a result the contribution of the aligned jet model (AJM) [12] is small, at least at high energies. Actually, an explanation showing that the emission of many gluons suppresses the nonperturbative AJM-type configurations has been given by Gribov and Lipatov [21] more than two decade ago. They showed that the emission of multi gluons generates a Sudakov form factor which suppresses the AJM-like contributions. Note that the result of the  $z$  integration is very important for the understanding of our approach since it justifies our idea that  $M^2$  is a good measure of the typical distances involved in the process. Indeed,  $r_{\perp}^2 \propto \frac{1}{M^2}$  holds only for  $z \sim 1$  (see (29)). These estimates have been made for the total cross section. For exclusive channels the situation is quite different. For example, for the diffractive dissociation in DIS, induced by a transverse polarized photon, the typical distances are rather large and do not depend on the value of the mass in the Gribov's formula.

For heavy quarks, the diagrams of Fig. 4 give

$$\begin{aligned} \sigma_{QQ}^{hard} &= \frac{\alpha_{em}}{3\pi} 2\pi^2 \int_{4m_Q^2}^{\infty} \frac{dM^2 R^{QQ}(M^2)}{Q^2 + M^2} \int_{Q_0^2}^{\infty} \frac{d\tilde{M}^2}{\tilde{M}^4} \\ &\times \alpha_S \left( \frac{\tilde{M}^2}{4} \right) x G \left( x, \frac{\tilde{M}^2}{4} \right) \left\{ \frac{M^2 - Q^2}{M^2 + Q^2} \right. \\ &\left. + \frac{Q^2 + \tilde{M}^2 - M^2}{\sqrt{(Q^2 + M^2 + \tilde{M}^2)^2 - 4(M^2 - 4m_Q^2)\tilde{M}^2}} \right\} \end{aligned} \quad (44)$$

where  $R^{QQ}$  is the heavy quark contribution to the ratio in (3), and  $m_Q$  is the mass of the heavy quark. In (44) we have assumed that the quark is heavy enough to be described in pQCD without any contribution of the "soft" processes. In the above formulae  $x = \frac{Q^2 + M^2}{W^2}$ , and  $W$  is the energy of the photon-nucleon interaction.

### 3.3 A model for the "soft" interactions

Our model for the "soft" interactions is based on (34). We observe that our discussion on the time structure of the

photon-hadron interaction does not depend on any specific properties of QCD, and can be considered, therefore, as a main feature of the parton model approach to high energy photon induced interactions (see [13]). It means that, the approximation  $z = z'$  in Fig. 1 applies also for the "soft" interactions of our model.

In the parton model [13], as well as in the high energy phenomenology [14], the "soft" processes at high energy can be described by the exchange of a soft Pomeron which has the property of Regge factorization [15]

$$\sigma_P(s, M, M') = g_P(M, M') G_P \left( \frac{s}{M^2} \right)^{\alpha_P(0)-1},$$

where  $\alpha_P(t)$  is the Pomeron trajectory and  $g_P(M, M')$  and  $G_P$  are vertices of the Pomeron interaction with the quark-antiquark pair and with the proton respectively. Substituting this equation in (11) one can see that only the photon wave function depends on  $z$ . This integral is convergent and  $z$  is typically about unity also for a photon with large virtuality. Coming back to (37) one can see that  $M'$  could be different from  $M$  only if  $k_{2\perp} \gg k_{1\perp}$  (or  $k_{2\perp} \ll k_{1\perp}$ ). On the other hand, in the parton model the typical transverse momenta ( $l_{\perp}$  in Fig. 4) are of the order of the "soft" scale, i.e. about 1 GeV. Therefore, in a photon-hadron interaction we expect that the value of  $M'$  cannot be much larger than the value of  $M$ . The success of the additive quark model (AQM) (see the first diagram in Fig. 4) in the description of the high energy scattering (see [14]) supports our assumption that the difference ( $M' - M$ ) is much smaller than the transverse momentum scale for the Pomeron.

We can, therefore, rewrite the general Gribov formula of (7) in the form

$$\begin{aligned} \sigma^{soft}(\gamma^* N) &= \frac{\alpha_{em}}{3\pi} \int_{4m_{\pi}}^{M_0^2} \frac{R(M^2) M^2 dM^2}{(Q^2 + M^2)^2} \sigma_{M^2 N}(s) \\ &\times \int_{-M}^M \frac{M d\Delta M}{M^2} \frac{g_P(M, M')}{g_P(M, M)} \frac{M^2 + Q^2}{(M + \Delta M)^2 + Q^2} \\ &= \frac{\alpha_{em}}{3\pi} \int_{4m_{\pi}}^{M_0^2} \frac{R(M^2) M^2 dM^2}{(Q^2 + M^2)^2} \tilde{\sigma}_{M^2 N}(s), \end{aligned} \quad (45)$$

where  $\Delta M = M' - M$ .

Note that the  $\Delta M$  integration is particular to photon induced reactions and is, obviously absent in the case of hadron-hadron collisions. This correction, as well as other relevant corrections, are absorbed in our definition of  $\tilde{\sigma}_{M^2 n}$  in (45). In light of the above discussion, we choose (34) and/or (45) as the master formula for our description of the "soft" contribution.

The quantities appearing in (34) which need to be specified are the ratio  $R(M^2)$ , and the interaction cross section of a hadronic system with mass  $M$  with the target ( $\sigma_{M^2 N}(s)$  in (34)). Although, there is experimental data for  $R(M^2)$  (see [17]), we have used the parameterization of [18] for  $R(M^2)$ <sup>4</sup>. The two main ingredients of this parameterization, reproducing the experimental data, are

<sup>4</sup> We thank E. Gurvich for drawing our attention to [18]



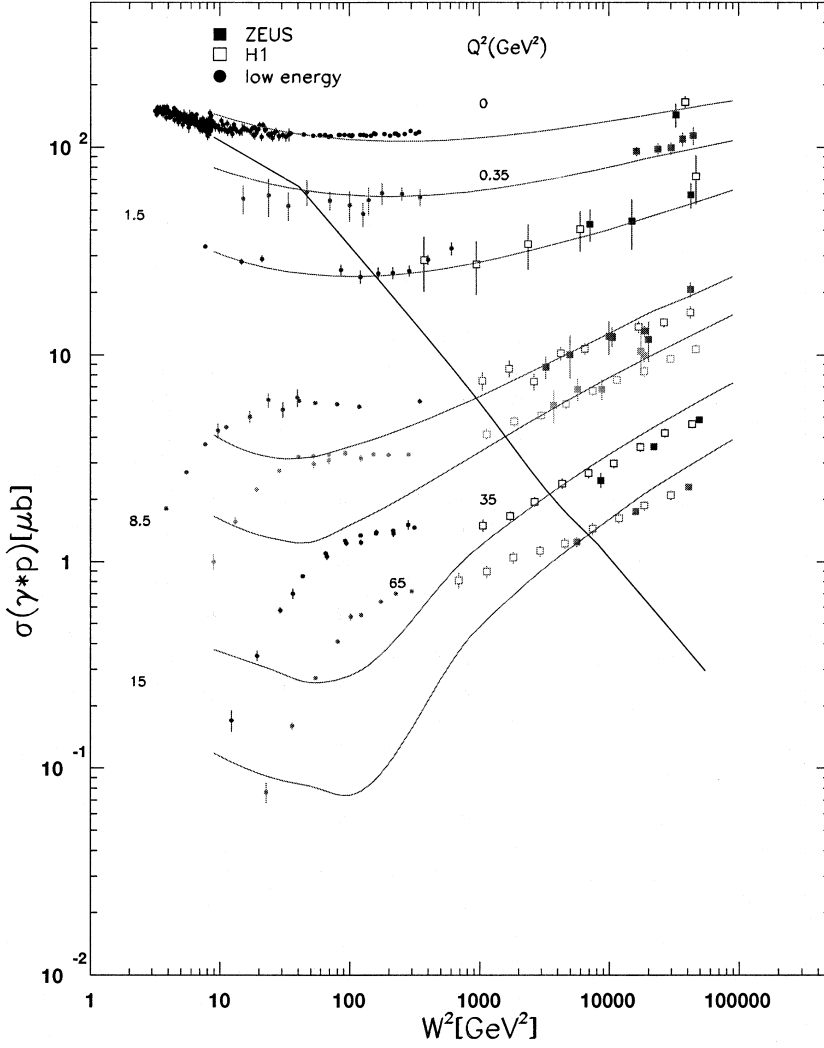


**Fig. 5.** The comparison of the experiment data (see [24] and references therein) for  $\sigma(\gamma^*p)$  and our calculation, using (49). The diagonal line indicates the boundary for  $x = 10^{-2}$

the resonance contribution and the background, which at high masses approaches the QCD result ( $R(M^2) \rightarrow R_\infty$ ). We approximate  $\tilde{\sigma}_{M^2N}$  in the resonance region by

$$\sigma_R = \kappa \frac{1}{2} (\sigma(\pi^+p) + \sigma(\pi^-p)) \quad (46)$$

where we use the Donnachie-Landshoff Reggeon parameterization [14] for the cross section of pion-proton interaction,

$$\sigma_R = \kappa \left[ A \left( \frac{s}{s_0} \right)^{\alpha_P(0)-1} + B \left( \frac{s}{s_0} \right)^{\alpha_R(0)-1} \right], \quad (47)$$

with a Pomeron and Reggeon trajectory intercepts of  $\alpha_P(0)=1.079$  and  $\alpha_R(0)=0.55$ ;  $s_0=1 \text{ GeV}^2$ ;  $A=13.7 \text{ mb}$  and  $B=31.9 \text{ mb}$ . We introduce a rescaling constant  $\kappa$  as a parameter in (46) and (47).  $\kappa = 1$  corresponds to a simplified AQM where the integrand is taken at  $\Delta M = 0$  and first order corrections of  $\frac{\Delta M}{M}$  and  $\frac{\Delta M}{m_G}$ , where  $m_G$  is the typical scale of the soft Pomeron, are neglected. This is discussed further in Sect. 3.4.

To describe the interaction of the background contribution in  $R(M^2)$ , we need to determine the correct energy

variable for the interaction of the hadronic system of mass  $M$  with the target. We suggest to replace the variable  $\frac{s}{s_0}$  by  $\frac{1}{x_M}$ , where  $x_M = \frac{M^2}{s}$ . In other words, we replace (47) by

$$\tilde{\sigma}_{M^2N} = \kappa \left[ A' \left( \frac{1}{x_M} \right)^{\alpha_P(0)-1} + B' \left( \frac{1}{x_M} \right)^{\alpha_R(0)-1} \right], \quad (48)$$

where  $A' = 13.1 \text{ mb}$  and  $B' = 41.08 \text{ mb}$ . The values of  $A'$  and  $B'$  were chosen so that (47) for the  $\rho$  meson-proton interaction is valid. The variable  $x_M$  is not unique, but it correctly describes the high energy interaction, in all parton-like models in the region of large mass  $M$  (see [11] for example).

### 3.4 Comparison with the experimental data

To compare with the experimental data, we calculate the total cross section of the photon-proton interaction using the following formula

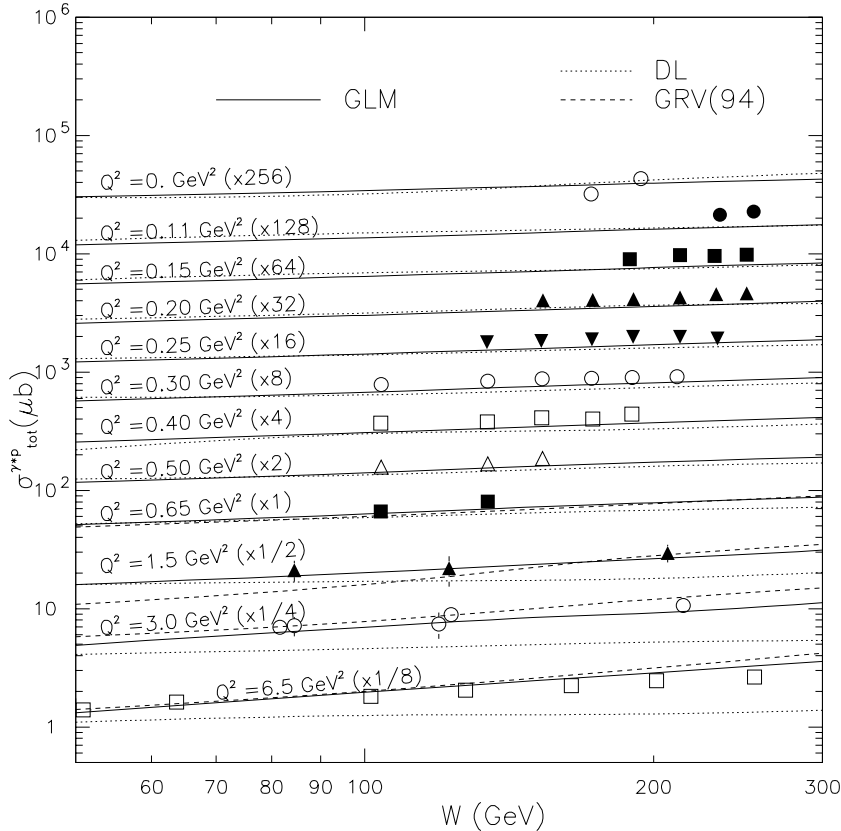


**Fig. 6.** Low  $Q^2$  and high  $W$  data from ZEUS (see [25]), compared to our predictions (solid lines), Donnachie-Landshoff approach [14] (dotted lines) and the GRV parameterization [16] (dashed lines)

$$\sigma(\gamma * p) = \sigma^{soft}(\text{Eq. (34), Eq. (48)}) + \sigma_{\bar{q}q}^{hard}(\text{Eq. (40)}) + \sigma_{QQ}^{hard}(\text{Eq. (44)}). \quad (49)$$

Equation (49) depends on two free parameters:  $\kappa$  and  $M_0^2$  and the input gluon distribution  $xG(x, \frac{\bar{M}^2}{4})$ . In Fig. 5 we plot  $\sigma(\gamma * p)$  as a function of  $W^2$  for various values of  $Q^2$  and compare with the relevant experimental data. In our calculations we have used the GRV parameterization [16] in higher order of pQCD (GRVHO). We have chosen the parameters  $\kappa = 0.6$  and  $M_0^2 = 5 \text{ GeV}^2$  so as to obtain a reasonable reproduction of the data.

As can be seen from Fig. 5, we obtain a good fit for the low  $Q^2$  data over the entire  $W$  range. However, at  $Q^2$  higher than a few  $\text{GeV}^2$ , our description of the data is deficient in as much as we are not in agreement with the low energy experimental points and our predicted high energy behaviour is steeper than the data. Below we elaborate on these features as well as on some important details of the suggested model.

1. With only two free parameters, we manage to reproduce the energy dependence for real photoproduction and DIS with  $Q^2 < 8 \text{ GeV}^2$  cross sections. This is shown in Fig. 6 where we compare the recent high-energy-low  $Q^2$  ZEUS data [25] with the predictions of our model. Our results compare favorably with the Donnachie-Landshoff [14] and GRV [16] parameterizations.

2. The fact that we are unable to reproduce the low energy behaviour of the higher  $Q^2$  ( $x > 10^{-2}$ ) data is not surprising. These data correspond to higher  $x$  values

for which the two gluon approach to DIS is insufficient. In Fig. 5 we show the line corresponding to  $x = 0.01$  which illustrates this point. Clearly for high  $x$  (low  $W$ ) one should also include the contribution coming from the  $Q^2$  evolution of the quark distribution as a part of the pQCD description of DIS. We discuss below how to expand our formalism so as to include this input as well. The fit can also be improved by the utilization of other input parton distributions which are less steep than GRVHO in the small  $x$  limit.

3. An unexpected feature of our results is that we require a value of  $\kappa = 0.6$  to rescale the AQM estimate of the “soft” contribution. As we have noted, this value of  $\kappa$  reflects the need to integrate over  $\Delta M$  which is particular to photoproduction and DIS and does not appear in hadron-hadron scattering, where the AQM has been checked experimentally. Our result is different from VDM [19], where in order to describe the experimental data, one has to assume that the vector meson-nucleon cross section is bigger than the AQM estimates. This difference arises from the background contribution that is neglected in the VDM approach. It should be stressed that such a contribution, which is included in our parameterization of  $R(M^2)$ , is needed to reproduce the  $Q^2$ -dependence, which is much smoother than the VDM prediction. In addition to uncertainties from the  $\Delta M$  integration we also see at least two reasons leading to a value of  $\kappa$  smaller than unity. Our evaluation suggests that using the approximate formula of [18] we overestimate the experimental data by about 10% ( $\kappa \approx 0.9$  from this source). The second source

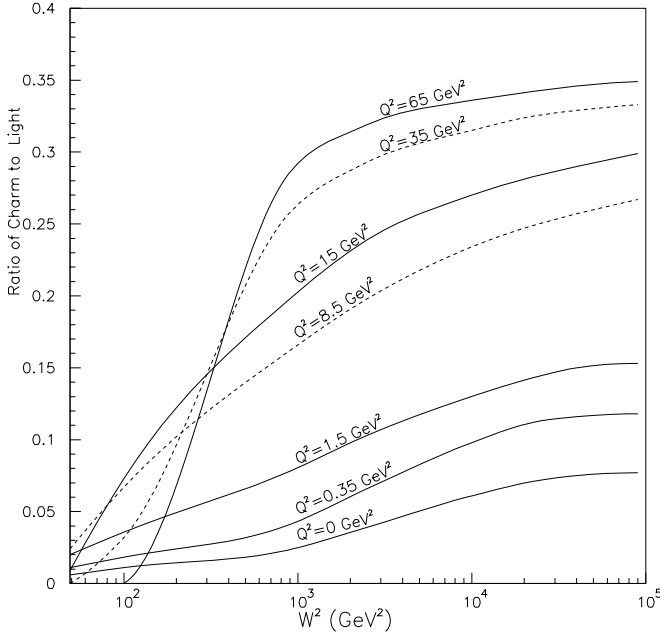


**Fig. 7.** The ratio  $R_{LIGHT}^{CHARM} = \frac{\sigma(\text{charm quarks})}{\sigma(\text{light quarks})}$  as function of  $W^2$  for different values of  $Q^2$

is the need for shadowing corrections (SC). SC definitely diminish the value of the cross section. We can estimate the SC from the value of the diffractive dissociation cross section, using the AGK cutting rules [20], which relates the SC to the total cross section, namely,  $\Delta\sigma^{SC} = \sigma^{DD}$ , where  $\sigma = \sigma^{AQM} - \Delta\sigma^{SC}$ . The experimental value of the diffractive cross section is about 15%, both from real photoproduction and from pion-proton interaction. These two sources suggest a value of  $\kappa \approx 0.7$  to which an additional 15% reduction is added due to the  $\Delta M$  integration<sup>5</sup>.

4. The inclusion of heavy quark contribution is important. In Fig. 7 we plot the ratio  $R_{LIGHT}^{CHARM} = \frac{\sigma(\text{charm quarks})}{\sigma(\text{light quarks})}$  as a function of energy at different values of  $Q^2$ . This ratio is rather small for real photoproduction, reaching 5% at high energies. For large values of  $Q^2$  the ratio approaches 30-35% at high energies  $W \geq 30 \text{ GeV}$ .

In general, our model provides a very simple approach to incorporate the “soft” and “hard” components of photoproduction and DIS. In the detailed fit of the data we observe two features that we consider to be rather general.

1. The high energy “hard” contribution turns out to be sizable, even for  $Q^2 = 0$ . To illustrate, how important the “hard” contribution is in our formalism, we plot in Fig. 8 the ratio  $R_S^H = \frac{\sigma^{hard}(\gamma^*p)}{\sigma^{soft}(\gamma^*p)}$ . One can see that for  $Q^2 = 0$ ,  $R_S^H \approx 1\%$  at  $W = 10 \text{ GeV}$  and it grows to  $R_S^H \approx 15\%$  at  $W = 300 \text{ GeV}$  ( $s = W^2$ ). This increase is sufficiently large, that it alone may account for the experimentally observed increase in the energy dependence of the total cross section, for real photoproduction. In other words, it is possible to fit the experimental data assuming that the

<sup>5</sup> Note, that a similar suppression is required in a GVDM description of DIS [26]

“soft” Pomeron (see (47)) has an intercept which is equal to unity ( $\alpha_P(0)=1$ ).

Our result suggests a possible and interesting interpretation for the origin of the experimentally observed increase of the total cross sections for hadron-hadron interactions. As for each hadron we also have a contribution of the “hard” process to the total cross section, due to the probability that two quarks approach each other at a sufficiently small distance. The probability for this “hard” process is controlled by the respective wave functions of the interacting hadrons.

2. We find contamination of the “hard” processes by the “soft” ones. For example, at  $Q^2 = 15 \text{ GeV}^2$  which is usually considered a large value for  $Q^2$ , the ratio  $R_H^S = \frac{\sigma^{soft}(\gamma^*p)}{\sigma^{hard}(\gamma^*p)}$  changes from 1 at  $W = 30 \text{ GeV}$  to 0.2 at  $W = 300 \text{ GeV}$ . Even at  $Q^2 = 65 \text{ GeV}^2$ ,  $R_H^S$  is about 0.12 at  $W = 100 \text{ GeV}$ . The above results, lead one to view DIS in a new light, and provide a basis for a better understanding of what is meant by small distances or high photon virtualities.

### 3.5 A generalization of our model to larger $x$

The generalization is based on (40), utilizing the fact that for the DGLAP [21] evolution equation the following equation holds in the region of small  $x$  (see [22] for example)

$$\frac{\partial F_2^{DGLAP}}{\partial \ln(Q^2/A^2)} = \frac{2\alpha_S}{9\pi} x G^{DGLAP}(x, Q^2). \quad (50)$$

We suggest replacing  $\alpha_S x G(x, Q^2)$  in (40) by  $\frac{\partial F_2^{DGLAP}}{\partial \ln(Q^2/A^2)}$  and use this generalized formula for DIS, even in the region of  $x$  not very small. Note, that for  $x$  not too small, we obtain (see [22] for example) a more general formula for  $\frac{\partial F_2^{DGLAP}}{\partial \ln(Q^2/A^2)}$  than (50) which includes the quark densities. After doing so, (40) reduces to the form

$$\begin{aligned} \sigma^{hard} = & 3\pi^2 \alpha_{em} \int_{M_0^2}^{\infty} \frac{R(M^2) dM^2}{Q^2 + M^2} \\ & \times \int_0^{\infty} \frac{d\tilde{M}^2}{\tilde{M}^2} \frac{\partial F_2^{DGLAP}(x, \frac{\tilde{M}^2}{4})}{\partial \tilde{M}^2} \\ & \times \left\{ \frac{M^2 - Q^2}{M^2 + Q^2} \right. \\ & \left. + \frac{Q^2 + \tilde{M}^2 - M^2}{\sqrt{(Q^2 + M^2 + \tilde{M}^2)^2 - 4M^2\tilde{M}^2}} \right\}. \quad (51) \end{aligned}$$

Integrating (51) by parts one obtains

$$\begin{aligned} \sigma^{hard} = & 3\pi^2 \alpha_{em} \int_{M_0^2}^{\infty} \frac{R(M^2) dM^2}{Q^2 + M^2} \\ & \times \int_0^{\infty} \frac{d\tilde{M}^2}{\tilde{M}^4} F_2^{DGLAP} \left( x, \frac{\tilde{M}^2}{4} \right) \end{aligned}$$

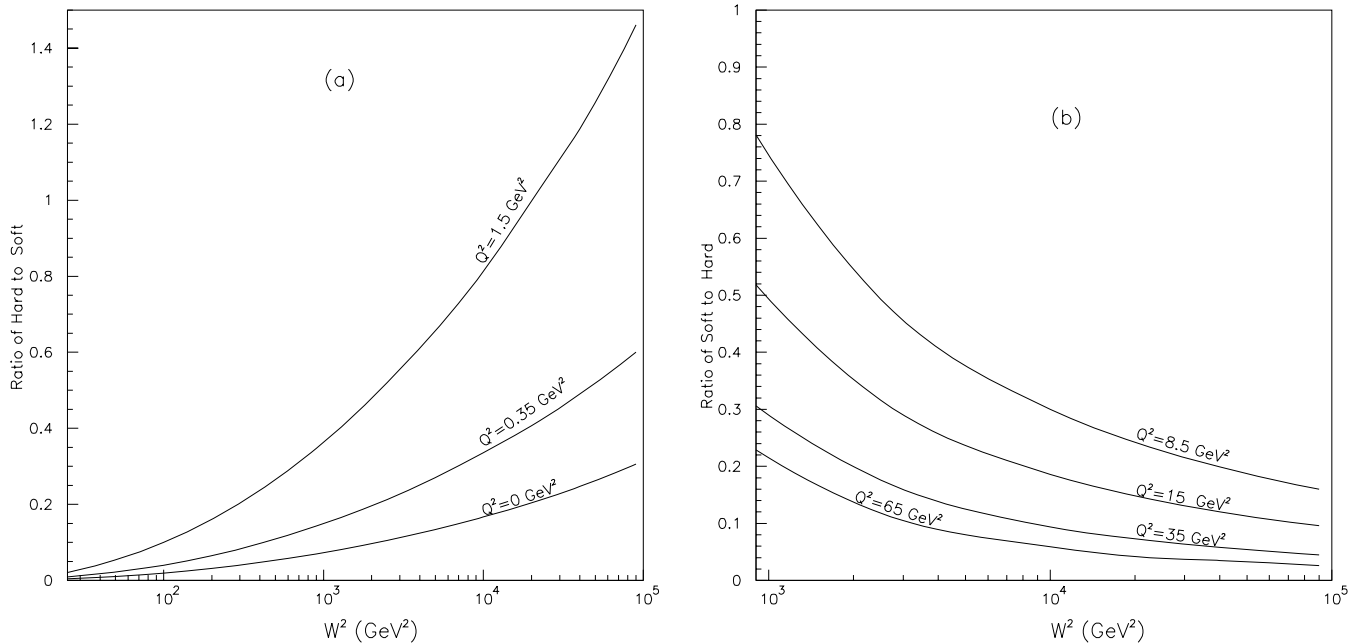


**Fig. 8.** The ratios **a**  $R_S^H = \frac{\sigma_{hard}(\gamma^*p)}{\sigma_{soft}(\gamma^*p)}$  and **b**  $R_H^S = \frac{\sigma_{soft}(\gamma^*p)}{\sigma_{hard}(\gamma^*p)}$  as function of  $W^2$  for different values of  $Q^2$

$$\left. \begin{aligned} & \times \left\{ \frac{M^2 - Q^2}{M^2 + Q^2} \right. \\ & + \frac{Q^2 + \tilde{M}^2 - M^2}{\sqrt{(Q^2 + M^2 + \tilde{M}^2)^2 - 4M^2\tilde{M}^2}} \\ & \left. - \frac{4Q^2M^2\tilde{M}^2}{\sqrt{(Q^2 + M^2 + \tilde{M}^2)^2 - 4M^2\tilde{M}^2}} \right\}. \end{aligned} \right\} (52)$$

Actually, a formula of the same type as (52) was first suggested by Badelek and Kwiecinski [23], but using our formalism we obtain quite a different result. We can consider (52) as a generalization of the Badelek-Kwiecinski approach. In addition to the resonances we have also included the background contribution, and obtain the contributions of both “soft” and “hard” processes by integrating over  $M^2$  and  $\tilde{M}^2$  in (52).

Numerical results pertaining to (52) will be published separately.

## 4 Conclusions

We have achieved two goals in this paper:

1. We provide an explanation of how and why the short distance (“hard”) interaction, calculable in pQCD, provides a mass cutoff in the Gribov’s formula for photon-hadron collisions. We have shown that the Gribov bound (see (4)) given in [5], overestimates the photon-hadron cross section, and should be replaced by a more restrictive limit, as derived in this paper (see (31),(32) and (33)). At fixed  $Q^2$  as  $W \rightarrow \infty$  our bound is  $\sigma(\gamma^*p) \leq C'(\ln \frac{1}{x})^{\frac{5}{2}}$ .

2. We developed a simple model which consists of two contributions: “soft” and “hard”. The “soft” term descri-

bes the long distance contribution, while the “hard” term is related only to the short distance interaction controlled by pQCD (and the DGLAP evolution equation [21]). This simple model with only two parameters provides a good description of the available experimental data over a wide range of  $W$  and  $Q^2 < 8 \text{ GeV}^2$ . We have suggested a technique of how to improve the high  $Q^2$  results at sufficiently small values of energy  $W$ .

Examining our model we found two interesting features that may be more general:

- a) Short distance effects contribute even at  $Q^2 = 0$  for high energies. The contribution is sufficient to explain the energy rise of the total cross section for photoproduction, which has been interpreted as an argument that the “soft” Pomeron has an intercept larger than 1 (see [14]). This result encourages us to reconsider this widely held explanation, and to estimate the contributions of the “hard” processes to the growth of hadron-hadron cross sections, with increasing energy.

- b) The long distance processes contribute to the total cross section even at rather large values of  $Q^2$ . For example, at  $Q^2 = 65 \text{ GeV}^2$  and  $W = 100 \text{ GeV}$  they are responsible for 10% of the total cross section. This observation can be very important for understanding the energy dependence, as well as the value of the cross sections of other processes such as diffractive dissociation, inclusive production etc. We propose to examine these processes in the near future using the same approach.

Our approach is not in contradiction with the usual description of “hard” processes, based on the DGLAP evolution equations with initial nonperturbative parton densities at  $Q^2 = Q_0^2$ . However, we significantly enlarged the region of applicability of such an approach, noting that the quark-antiquark pair with large mass can be treated in

pQCD even at  $Q^2 = 0$ . It allowed us to separate the non-perturbative contribution in a different way than usually done and to calculate a part of the initial parton densities at  $Q^2 = Q_0^2$  in pQCD.

In general, the model suggested allows one to discuss the interface between long and short distance processes, not only on the qualitative level but also on a quantitative one. We are of the opinion that our model incorporates what is known, both theoretically and phenomenologically about “soft” and “hard” physics, and provides a method to estimate the different contributions to a variety of processes. It also allows one to specify the kinematic region where the “hard” contribution dominates, and to calculate it within the framework of pQCD.

*Acknowledgements.* We would like to thank our colleagues at Tel Aviv, E. Gurvich for providing us with a program to evaluate  $R(M^2)$  and A. Levy for making his file containing the experimental data on  $\sigma(\gamma^*p)$  available to us. E.G. and E.L. would like to acknowledge the kind hospitality of the Theory Group at DESY where this paper was completed. U.M. thanks LAFEX-CBPF (Rio de Janeiro) for their hospitality and support. This research was partially supported by THE ISRAEL SCIENCE FOUNDATION founded by the Israel Academy of Sciences and Humanities.

## References

1. M. Froissart: Phys. Rev. **123** (1961) 1053;  
A. Martin: “Scattering Theory: Unitarity, Analyticity and Crossing”, Lecture notes in Physics, Springer-Verlag, Berlin-Heidelberg-New York (1969)
2. E. Gotsman, E. Levin, U. Maor: Phys. Lett. **B309** (1993) 199; Phys. Rev. **D49** (1994) R4321
3. CDF collaboration, F. Abe et al.: Phys. Rev. **D50** (1994) 5535; D. Goulianos: Phys. Lett. **B358** (1995) 379
4. V.N. Gribov: Sov. Phys. JETP **30** (1970) 709
5. H. Abramowicz, L. Frankfurt, M. Strikman: DESY 95-047; hep-ph/9503437
6. E. Gotsman, E. Levin, U. Maor: Phys. Lett. **B403** (1997) 120
7. E.M. Levin, M.G. Ryskin: Sov. J. Nucl. Phys. **45** (1987) 150
8. A.H. Mueller: Nucl. Phys. **B335** (1990) 115
9. N.N. Nikolaev, B.G. Zakharov: Phys. Lett. **B260** (1991) 414, Z. Phys. **C49** (1991) 607, Z. Phys. **C53** (1992) 331
10. A.L. Ayala, M.B. Gay Ducati, E.M. Levin: Phys. Lett. **B388** (1996) 188
11. L.V. Gribov, E.M. Levin, M.G. Ryskin: Phys. Rep. **100** (1983) 1
12. J.D. Bjorken: Proceedings of the International Symposium on Electron and Photon Interaction at High Energy, Cornell, 1971; L.L. Frankfurt, M.I. Strikman: Phys. Rep. **160C** (1988) 235
13. R. Feynman: “Photon-hadron interaction”, Benjamin, 1972
14. A. Donnachie, P.V. Landshoff: Nucl. Phys. **B244** (1984) 322, Nucl. Phys. **B267** (1986) 690, Phys. Lett. **B296** (1992) 227, Z. Phys. **C61** (1994) 139
15. P.D.B. Collins: “An introduction to Regge theory and High energy physics”, Cambridge U.P., 1977
16. M. Gluck, E. Reya, A. Vogt: Z. Phys. **C53** (1992) 127
17. Particle Data Group, R.M. Barnett et al.: Phys. Rev. **D54** (1996) 1
18. R.B. Nevzorov, A.V. Novikov, M.I. Vysotsky: JETP Lett. **60** (1994) 399; hep-ph/9405350
19. T.H. Bauer, R.D. Spital, D.R. Yennie, F.M. Pipkin: Rev. of Mod. Phys. **50** (1978) 261
20. V.A. Abramovski, V.N. Gribov, O.V. Kancheli: Sov. J. Nucl. Phys. **18** (1973) 308
21. V.N. Gribov, L.N. Lipatov: Sov. J. Nucl. Phys. **15** (1972) 438; L.N. Lipatov: Yad. Fiz. **20** (1974) 181; G. Altarelli, G. Parisi: Nucl. Phys. **B126** (1977) 298; Yu.L. Dokshitzer: Sov. Phys. JETP **46** (1977) 641
22. R.K. Ellis, Z. Kunzst, E.M. Levin: Nucl. Phys. **B420** (1994) 517
23. B. Badelek, J. Kwiecinski: Z. Phys. **C43** (1989) 251, Phys. Lett. **B295** (1992) 263, Phys. Rev. **D50** (1994) R4
24. H. Abramowicz: Plenary talk at ICHEP’96, Warsaw, July 1996, in Proceedings of the XXVIII International Conference on High Energy Physics, eds. Z. Ajduk, A.K. Wroblewski, WS, p53
25. ZEUS collaboration, J. Breitweg et al.: DESY 97-135, July 1997, hep-ex /9707025
26. H. Fraas, R.J. Read, D. Schildknecht: Nucl. Phys. **B86** (1975) 364, **B88** (1975) 301